Energy dependence of pion double charge exchange

Mutazz Nuseirat and M. A. K. Lodhi
Texas Tech University, Lubbock, Texas 79409

M. O. El-Ghossain
The Islamic University of Gaza, Gaza

W. R. Gibbs
New Mexico State University, Las Cruces, New Mexico 88003

W. B. Kaufmann
Arizona State University, Tempe, Arizona 85287

(Received 1 June 1998)

The energy dependence of forward angle pion double charge exchange is calculated in the energy range of 0–250 MeV. The most striking feature is a peak around 40 MeV which is in excellent agreement with the data when distorted waves obtained from a realistic optical model are used. Two possible short-range corrections to the reaction mechanism are addressed. [S0556-2813(98)07410-X]

PACS number(s): 25.80.Gn, 24.10.Ht

I. INTRODUCTION

Pion double charge exchange (DCX) on nuclear targets has been extensively studied, both experimentally and theoretically, throughout the last two decades. Because at least two nucleons must be involved in the process, the study of DCX is a natural tool for exploring nucleon-nucleon correlations. In the course of these studies at low energies, a prominent peak in the (π^+,π^-) cross section in the neighborhood of $T_\pi=40$ MeV was observed by a number of experimental groups [1–3]. The peak occurs for a variety of nuclear targets and seemingly independent of the final state.

It has been claimed [3] that this peak provides evidence for the existence of a dibaryon at this energy. Before accepting such an interpretation, it is important to consider the more conventional ones. In this paper we will show (as has been previously suggested [4–8]) that such a peak arises naturally because of the pion propagation in the conventional ''sequential process,'' in which DCX occurs through two successive πN charge exchange reactions on two neutrons [9–11]. Our calculation is based on the conventional distorted-wave impulse approximation (DWIA), which we briefly outline. Calculations of the reaction leading to both the double isobaric analog state (DIAS) and the ground state are made.

While other reaction mechanisms have been studied [7,12–15], we treat DCX as a two-step sequential process. It is generally accepted now that this is likely to be the dominant mechanism for the types of transitions treated here although the other mechanisms could alter the picture somewhat. In contrast to most nuclear reaction calculations, the DCX amplitude must be evaluated in second order so that we will need to compute, not only the distorted incoming (π^+) and outgoing (π^-) pion wave functions, but also the distorted π^0 Green function, which describes the propagation of the pion between two nucleons.

The distorted pion wave functions and Green's functions are computed from truncated Klein-Gordon equations which incorporate the optical potentials for the initial $[\pi^+ + (Z,A)]$, final $[\pi^- + (Z+2,A)]$, and intermediate $[\pi^0 + (Z+1,A)]$ systems. In addition to the conventional optical potentials [16], we include imaginary effective potentials which model pion true absorption (annihilation). One of the major changes in the present calculation compared with previous work, involves the use of realistic pion elastic scattering wave functions. These new wave functions were obtained by including a new parametrization of the correction for pion true absorption to the potential, increasing the number of independent partial waves from two to six and fitting the remaining parameters to measured elastic scattering and reaction cross sections [17]. Since we use the distorted pion wave functions from these fits without modification the DCX cross sections obtained are predictions.

The π^0 Green function is less certain since it is calculated using the same theory for the external waves, but the state of the nucleus during the propagation of the neutral pion is not well defined, nor is it directly testable as are the external waves. We have chosen an effective nuclear excitation energy $(=0)$, and used closure over the intermediate nuclear states. The uncertainty in this ''closure approximation'' affects more greatly processes which lead to the analog final state, which involve longer π^0 propagation distances. The general DWIA procedure is outlined in Sec. II A, and the technique for the numerical solution is given in Appendix A. This intermediate distortion has been considered in a number of other works [9,18–21].

We have used somewhat realistic shell model wave functions for the initial ground state, the final ground state, and the final analog states. For the Ca isotopes we use the seniority model within the $f_{7/2}$ shell as well as more accurate wave functions for the final ground states [22] as described in Sec. II B. In the seniority model DCX for all the isotopes is given in terms of two complex amplitudes. One amplitude is primarily sensitive to the short-range correlation of the valence

nucleons and spin dependence of the DCX amplitude; the other amplitude to the long-range behavior. Furthermore, the relative importance of these two amplitudes depends very much on the pion energy. For ^{14}C we use a mixture of $(1p_{1/2})^2$ and $(1p_{3/2})^2$ configurations.

Aside from questions involving the propagation and the nuclear wave functions, there are those that surround the interaction operator itself. While this operator is taken to be two separate charge exchanges, the off-shell iteration involving two *p*-wave basic interactions creates a δ-function interaction [23] much as in the case of the nucleon-nucleon interaction [24]. The removal of this unphysical δ function provides a correction to the reaction operator. This δ function has been previously treated in the setting of pion propagation in a nuclear medium [25,26].

Once the very short range part of the interaction is considered, one is led to question the mechanism of the exchange of a neutral particle at very short distances. Indeed, once the nucleons are overlapping, it is possible that the reaction takes place on the level of quarks and gluons. Since the volume of the region of overlapping nucleons is not large, we may expect the effect to be small, but since we are able to enhance the sensitivity to the short range region, by choosing a particular transition, it becomes interesting to make an estimate of the size of an effect that might be caused by the static exchange of a single gluon.

II. SEQUENTIAL CALCULATION

A. DCX cross section calculation

The basic method used for the calculation of the DCX reaction is the same as that employed in a number of other presentations [9,2]. It involves the evaluation of the matrix element

$$M(\mathbf{k},\mathbf{k}')=\int d\mathbf{r}_1 d\mathbf{r}_2 \Phi_f^*(\mathbf{r}_1,\mathbf{r}_2)[\Psi_{\pi^-}^{*(-)}(\mathbf{k}',\mathbf{r}_2) f_2(\mathbf{q}_2,\mathbf{q}_2') G(\mathbf{r}_2,\mathbf{r}_1) f_1(\mathbf{q}_1',\mathbf{q}_1)\Psi_{\pi^+}^{(+)}(\mathbf{k},\mathbf{r}_1)]\Phi_i(\mathbf{r}_1,\mathbf{r}_2), \tag{1}$$

where the momenta $\mathbf{q}_1=(\hbar/i)\nabla_1$ and $\mathbf{q}_2=(\hbar/i)\nabla_2$ are operators on the conjugate coordinates in the pion wave functions $\Psi_{\pi^+}^{(+)}(\mathbf{k},\mathbf{r}_1)$ and $\Psi_{\pi^-}^{(-)}(\mathbf{k}',\mathbf{r}_2)$ and the primed values operate on the corresponding coordinates in the Green function, $G(\mathbf{r}_2,\mathbf{r}_1)$. The method for the evaluation of the effect of the operators is described in Appendix A.

The single charge exchange operators f_1 and f_2 are derived from the pion-nucleon amplitudes and are expressed in momentum space as

$$f(\mathbf{q},\mathbf{q}')=\lambda_0(E)v_0(q)v_0(q')+\lambda_1(E)\mathbf{q}\cdot\mathbf{q}'v_1(q)v_1(q') + \boldsymbol{\sigma}\cdot\mathbf{q}\times\mathbf{q}'\lambda_f(E)v_f(q)v_f(q'). \tag{2}$$

In the present calculation we take

$$v_0(q)=v_1(q)=v_f(q)=\frac{\Lambda^2+k^2}{\Lambda^2+q^2} \tag{3}$$

for the off-shell extension. A value of $\Lambda=400$ MeV/c was used in the calculations presented later. The λ's are obtained from the pion-nucleon phase shifts [27]. Representative values are given in Ref. [23]. An improved calculation might take the three ranges distinct, the three functions distinct, or better yet, a different function for each of the six pion-nucleon partial waves important in this energy region.

The functions $\Phi(\mathbf{r}_1,\mathbf{r}_2)$ are the wave functions of the two active nucleons. If there are more than two nucleons in the valence shell, such as is the case for ^{44}Ca and ^{48}Ca, an expansion in fractional parentage can be made as was treated in Ref. [9]. As is shown in that paper, the full amplitude can be decomposed into an uncorrelated amplitude, denoted as A, and a correlated amplitude, known as *B*. This separation is based on the seniority model, which is exact for a shell-model wave function consisting of a single shell with $j\leqslant\frac{7}{2}$ and maximal isospin $T=n/2$, where n is the number of nucleons in the shell. The seniority model is therefore exact for transitions from ^{42,44,48}Ca to the DIAS states of Ti. The ground states of ^{44,48}Ti have $T<n/2$, and for these nuclides the seniority model is an approximation. For these cases we have also used the more accurate McCullen-Bayman-Zamick (MBZ) [22] wave functions as discussed in the next section. For a nuclear wave function consisting of several orbitals, the concept of generalized seniority can be invoked and gives a similar result [28]. We will see that the separation into long- and short-range amplitudes plays an important role in understanding the energy dependence of DCX and hadronic propagation in the nucleus in general. The *B* amplitude comes from configurations in which the two nucleons are close together so that the propagation of the intermediate π^0 plays a small role, while in the amplitude *A* it is of significant importance.

The quantity in square brackets is the DCX operator. In Ref. [10] it was treated as arbitrary to investigate the behavior as a function of the isotopic number. In Ref. [23] this operator alone was treated in the plane-wave limit to derive its general characteristics. In Ref. [9] it was evaluated using the spectral representation for the Green function as explained in Appendix A. A much more effective method, first applied in Ref. [2], is to evaluate the Green function directly through numerical inversion of the Klein-Gordon operator, as is explained in Appendix A.

B. Nuclear wave functions

1. Calcium

The calcium isotopes provide a relatively good example of nuclei whose valence nucleons lie in a pure single shell. For this reason the wave functions are simple and reliable. In the seniority model, Eq. (1) can be used to express the am-

plitude to either the double isobaric analog state (DIAS) or the ground state in terms of two amplitudes, A and B, defined as [9]

$$A=F_0-\frac{1}{\Omega}\sum_{L=\text{odd}}F_L;\quad B=\sum_{L>0}F_L-\frac{(\Omega-1)}{\Omega}\sum_{L=\text{odd}}F_L, \tag{4}$$

with $\Omega=J+1/2$. If there is no spin dependence, i.e., $F_L=0$, L odd, then the amplitude A is the long-range (monopole) part of the DCX reaction while B is the short-range part. The analog and ground state transition amplitudes can be expressed in terms of these amplitudes:

$$\frac{d\sigma}{d\Omega}(\text{DIAS})=\frac{n(n-1)}{2}|A+XB|^2;$$

$$\frac{d\sigma}{d\Omega}(\text{g.s.})=\frac{n(n-1)}{2}|YB|^2, \tag{5}$$

where $n=2T$ is the number of valence neutrons and

$$X=\frac{(5-n)}{3(n-1)};\quad Y=\frac{4}{9(n-1)}\sqrt{(n-2)(10-n)}. \tag{6}$$

Explicitly, the cross sections for analog transitions on the calcium isotopes are given by

$$^{42}\text{Ca}:|A+B|^2;\quad ^{44}\text{Ca}:6|A+B/9|^2 \tag{7}$$

$$^{46}\text{Ca}:15|A-B/15|^2;\quad ^{48}\text{Ca}:28|A-B/7|^2. \tag{8}$$

2. Carbon wave functions

In this case the wave function is less well determined. There are believed to be important admixtures of the s and d shells as well as the $p_{1/2}$ and $p_{3/2}$ shells. For ^{14}C we take the two valence particles as two proton holes in a filled $1p$ shell. There are two independent basis vectors for a 0^+ state, which we choose as $1p_{3/2}$ and $1p_{1/2}$. Since the two configurations have similar energies, the ground state is better represented by a normalized combination of the two:

$$|\Phi\rangle=\cos\chi|(1p_{3/2})^2\rangle+\sin\chi|(1p_{1/2})^2\rangle, \tag{9}$$

where χ is the mixing angle [29]. We have calculated for χ equal to 66° which is essentially the value given by the p-state calculations of Cohen and Kurath [30].

III. RESULTS

Figure 1 shows a comparison of the distorted-wave calculation with the plane-wave version. From this figure we can get a general overview of the energy dependence. For the plane-wave calculations the cross section goes to zero at low energies because of the factor of momentum of the final state. Since the Q value of the reaction is -12.4 MeV in this case, the cross section must vanish below 12.4 MeV. The cross section rises rapidly and then decreases slightly before rising into the 33 resonance region. The plane-wave cross section is more than a factor of 100 larger than the measured cross section in this region.

The factors governing the distorted-wave calculation are very different. Just above threshold the energy of the final-state π^- is very small, as before, but with the attractive Coulomb interaction the cross section tends to infinity. This is a very low energy phenomenon, however, and the cross section quickly drops. Apparent in the calculation is an interference effect which causes the cross section to pass through zero around 20 MeV, after which it rises rapidly. This effect is shown on a larger scale in Fig. 2. The cross section will tend to infinity at the threshold because of the Coulomb interaction of the final π^- for all isotopes except ^{48}Ca, where the Q value is positive. Above 50 MeV the absorption of the pion (both types quasifree and ''true'') sets in and the cross section falls rapidly. In the region below 100

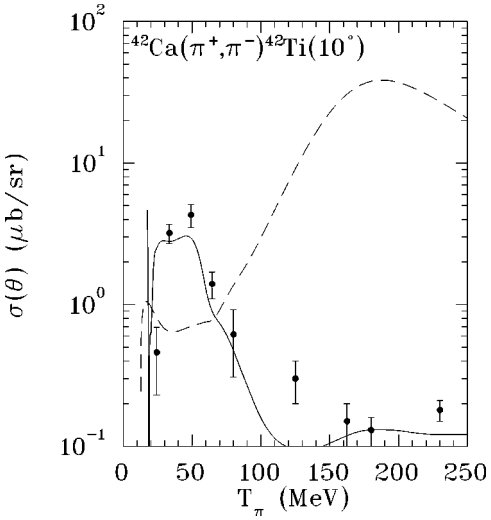

FIG. 1. Cross section for pion double charge exchange on ^{42}Ca leading to the analog state. The dotted curve displays the results of the calculation with plane waves and the solid curve with distorted waves.

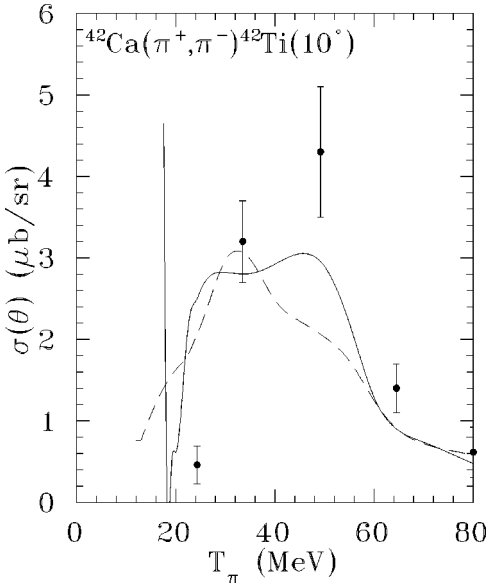

FIG. 2. Cross section for pion double charge exchange on ^{42}Ca leading to the analog state. The dotted curve displays the results of the calculation without a Coulomb potential and the solid curve includes it.

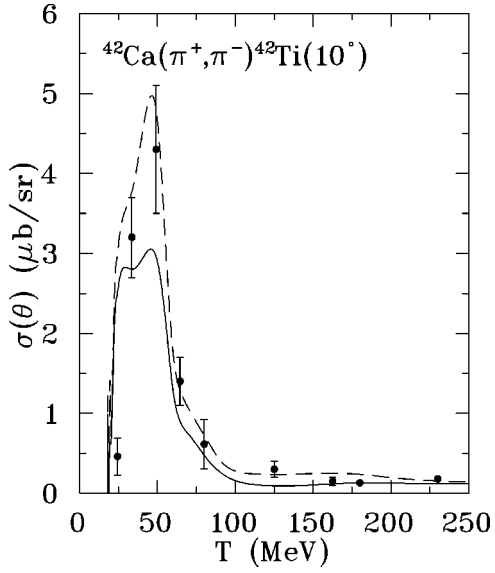

FIG. 3. Cross section for pion double charge exchange on ^{42}Ca leading to the analog state. The dotted curve displays the results of the calculation without the double spin flip included and the solid curve with.

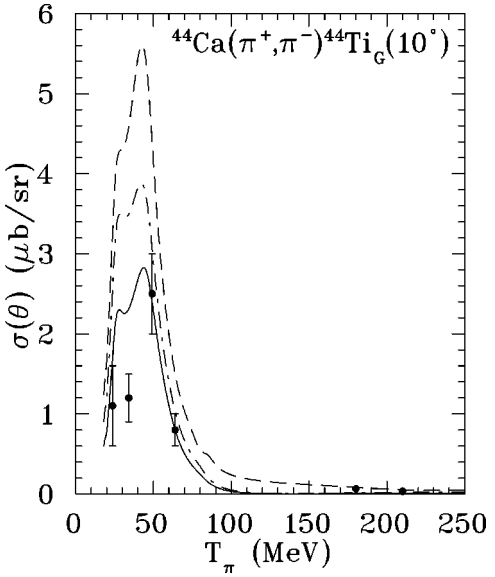

FIG. 4. Cross section for pion double charge exchange on ^{44}Ca leading to the ground state of ^{44}Ti. The dashed curve is calculated without double spin flip and with the seniority model, the dash-dot curve is calculated with double spin flip and the seniority model and the solid is calculated with double spin flip and the MBZ model [22].

MeV the resonances observed [17] in the elastic amplitudes also play a role.

In the figures to follow there is a comparison of the data [1,31–33] with calculations including and omitting the double spin flip (DSF) contribution. This is done because the DSF cancels against the term with no spin flip and reduces the cross section (in almost all cases). Since each of the transitions in the double spin flip is of a Gamow-Teller nature it is natural to ask if the suppression of this type of transition can play a role. We do not take a position on this issue but simply indicate the results with and without the DSF.

We distinguish three cases in the seniority model (1) B is the only amplitude, (2) B is the dominant amplitude, and (3) A and B enter on an equal footing. For ^{42}Ca the analog state is the ground state. The wave functions of the seniority model and those of MBZ are identical. Since $B \gg A$ over much of the energy range, B dominates. Figure 3 shows excellent agreement with the data.

Figures 4 and 5 show comparisons with the ground state transitions. Here B is the only amplitude, and the agreement with the data in the seniority model is very good. With the use of the more accurate MBZ wave functions, the agreement is excellent.

Figures 6 and 7 compare theory and data for the analog transitions for ^{44}Ca and ^{48}Ca. The strength of B for these two cases is reduced by a factor of 1/9 and $-1/7$, respectively, so that the contributions of A and B are comparable. In the case of ^{48}Ca there is a strong tendency for them to cancel. These cases show a great sensitivity to the values of amplitude A. For ^{48}Ca a much more complicated structure than a single peak results. It is interesting that the data points are consistent with it (at least below 150 MeV) although they cannot be said to imply such a structure *a priori*. Figure 8 shows the absolute values of amplitudes A and B for ^{48}Ca.

There are some interesting features to be compared with the model of a dibaryon causing this peak. There is a rapid rise of the cross section at low energies followed by flat-topped peak. The shape we predict is quite different from that of a single Breit-Wigner resonance. The qualitative agreement between predictions of the sequential model and the existing low-energy data supports the interpretation of this peak as an optical effect which does not require the introduction of a dibaryon resonance. Additional data at smaller energy intervals will be of great interest in determining the shapes of the low-energy peaks, and are essential in further clarifying their nature.

Figure 9 shows the calculation of the DCX reaction on

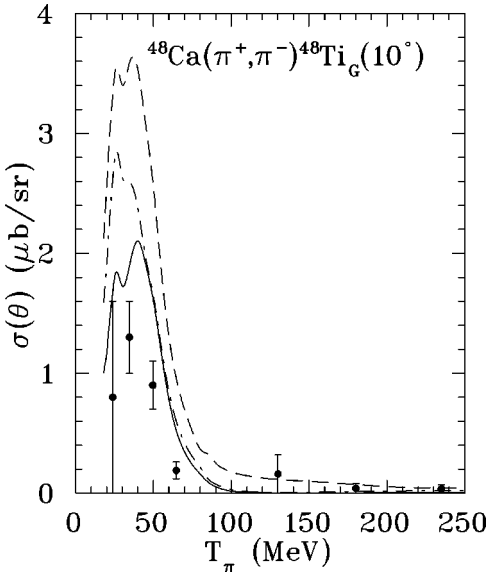

FIG. 5. Cross section for pion double charge exchange on ^{48}Ca leading to the ground state of ^{48}Ti. The meaning of the curves is the same as in Fig. 4.

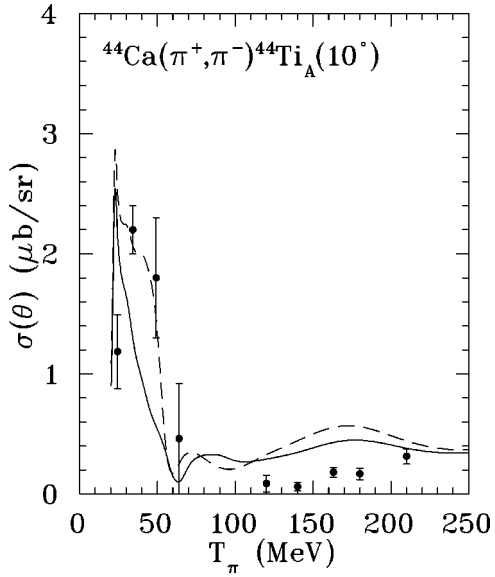

FIG. 6. Cross section for pion double charge exchange on ^{44}Ca leading to the analog state in ^{44}Ti. The meaning of the curves is the same as in Fig. 3.

^{14}C. The curves do not show the more detailed structure seen in the calcium isotopes, presumably because the resonances in the elastic phase shifts are less pronounced [17].

IV. SHORT RANGE CORRECTIONS

In this section we discuss possible corrections due to effects of short range on the order of the size of the nucleon or the pion.

A. The δ function in the DCX amplitude

The DCX operator resembles the one-pion-exchange potential between two nucleons in certain respects, since the dominant contribution to the pion-nucleon amplitude in this energy region is *p* wave in nature.

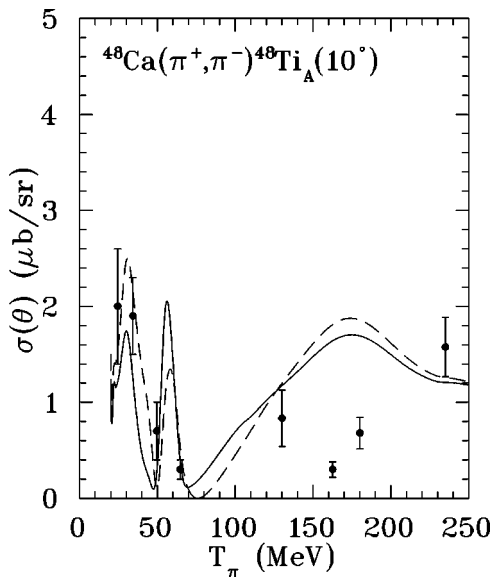

FIG. 7. Cross section for pion double charge exchange on ^{48}Ca leading to the analog state in ^{48}Ti. The meaning of the curves is the same as in Fig. 3.

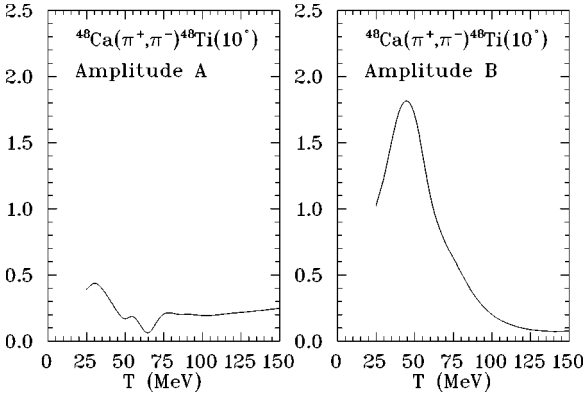

FIG. 8. Amplitudes *A* and *B* for pion double charge exchange on ^{48}Ca leading to the ground state of ^{48}Ti without double spin flip. The units are $(\mu b)^{1/2}$.

The appearance of the δ function in the DCX operator comes from the point of view of pointlike pion-quark coupling, where the pion-nucleon interaction extends over a finite region of space because of the distribution of quarks within the nucleon. This view is developed more fully in Ref. [24] for the case of *np* charge exchange. Since the δ function arises from the *p* wave-*p* wave part of the interaction, we need only consider that part of the DCX operator

$$F_{pp}(\mathbf{r}_1,\mathbf{r}_2)=(\alpha^2+k_0^2)^2\frac{\mathbf{k_2}\cdot\mathbf{q_2}}{(\alpha^2+q_2^2)}G(\mathbf{r_1},\mathbf{r_2})\frac{\mathbf{k_2}\cdot\mathbf{q_1}}{(\alpha^2+q_1^2)}, \tag{10}$$

where $\mathbf{q}_1$ and $\mathbf{q}_2$ are to be treated as operators on $\mathbf{r}_1$ and $\mathbf{r}_2$ in the Green function. Since we anticipate that the correction is of very short range, we will make (for the purposes of this correction only) the approximation that the neutral pion is

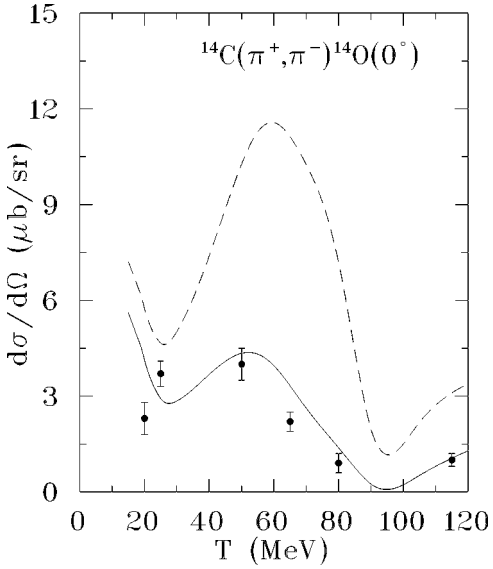

FIG. 9. Cross section for pion double charge exchange on ^{14}C leading to the ground state of ^{14}O. The solid curve has double spin flip included and no short range corrections while the dotted curve omits the double spin flip contribution.

undistorted in the intermediate state. In this case, expressing $G(\mathbf{r}_1,\mathbf{r}_2)$ in terms of its transform, we have

$$F_{pp}(\mathbf{r}_1,\mathbf{r}_2)\approx\alpha^2+k_0^2)^2\int\frac{d\mathbf{q}}{(2\pi)^3}\frac{\mathbf{k_2}\cdot\mathbf{q}\mathbf{k_1}\cdot\mathbf{q}}{(\alpha^2+q^2)^2}\frac{e^{i\mathbf{q}\cdot(\mathbf{r_1}-\mathbf{r_2})}}{q^2-k_0^2+i\epsilon} \tag{11}$$

$$=(\alpha^2+k_0^2)^2\int\frac{d\mathbf{q}}{(2\pi)^3}\frac{\mathbf{k_2}\cdot\hat{\mathbf{q}}\mathbf{k_1}\cdot\hat{\mathbf{q}}}{(\alpha^2+q^2)^2}e^{i\mathbf{q}\cdot(\mathbf{r_1}-\mathbf{r_2})}$$

$$\times\frac{q^2}{q^2-k_0^2+i\epsilon}. \tag{12}$$

The expansion of $\mathbf{k_2}\cdot\mathbf{q}\mathbf{k_1}\cdot\mathbf{q}$ will yield an s wave and a d wave part:

$$\mathbf{k_2}\cdot\mathbf{q}\mathbf{k_1}\cdot\mathbf{q}=\tfrac{1}{3}(\mathbf{k_2}\cdot\mathbf{k_1})q^2+\tfrac{1}{3}S_{12}, \tag{13}$$

where the tensor operator S_{12} is

$$S_{12}=[3(\mathbf{k_1}\cdot\mathbf{q})(\mathbf{k_2}\cdot\mathbf{q})-(\mathbf{k_1}\cdot\mathbf{k_2})q^2]. \tag{14}$$

Because the nucleons are assumed to be close to each other (for the purposes of this correction) we keep only the relative s wave. The s wave part of the p-wave-p-wave amplitude is given by

$$\tfrac{1}{3}\mathbf{k_2}\cdot\mathbf{k_1}(\alpha^2+k_0^2)^2\int\frac{d\mathbf{q}}{(2\pi)^3}\frac{e^{i\mathbf{q}\cdot(\mathbf{r_1}-\mathbf{r_2})}}{(\alpha^2+q^2)^2}\frac{q^2}{q^2-k_0^2+i\epsilon}. \tag{15}$$

As discussed in Ref. [24] there is a δ function at $\mathbf{r}_1=\mathbf{r}_2$ in Eq. (15) in the limit as $\alpha\to\infty$. This singularity is unphysical because of the finite size of the pion. If we neglect the interaction within the quark-quark range of less than the size of a pion (and then take the limit of the pion size going to zero) we find that the corrected interaction becomes

$$\to(\alpha^2+k_0^2)^2\,\tfrac{1}{3}\mathbf{k_2}\cdot\mathbf{k_1}$$

$$\times\int\frac{d\mathbf{q}}{(2\pi)^3}\frac{e^{i\mathbf{q}\cdot(\mathbf{r_1}-\mathbf{r_2})}}{(\alpha^2+q^2)^2}\left(\frac{q^2}{q^2-k_0^2+i\epsilon}-1\right). \tag{16}$$

Thus, the correction to the operator is

$$C_O=-\tfrac{1}{3}\mathbf{k_2}\cdot\mathbf{k_1}(\alpha^2+k_0^2)^2\int\frac{d\mathbf{q}}{(2\pi)^3}\frac{e^{i\mathbf{q}\cdot(\mathbf{r_1}-\mathbf{r_2})}}{(\alpha^2+q^2)^2} \tag{17}$$

$$=-\tfrac{1}{3}\mathbf{k_2}\cdot\mathbf{k_1}\sum Y_{L'}^{m'}(\hat{\mathbf{r}}_1)Y_{L'}^{M'*}(\hat{\mathbf{r}}_2)g_{L'}(r_1,r_2). \tag{18}$$

This integral can be evaluated by contour integration. The development of the expressions for the distorted waves is given in Appendix C.

B. One gluon exchange

In the preceding section the short-range quark-quark interaction was neglected. After the limit was taken, only the δ function was eliminated. One might believe, however, that for two quarks closer than the diameter of a pion the interaction would pass from that of pion exchange to one based on quark-gluon degrees of freedom in some continuous manner. The generation of this short-range interaction merits a thorough study, beyond the scope of the present paper. However, it is possible to make a rough estimate of the size of the effect by adopting results from calculations of the nucleon-nucleon case in the static limit [34]. The nonrelativistic two-body one-gluon-exchange (OGE) potential is expected to have the form

$$V_{\mathrm{OGE}}(\mathbf{r}_{ij})=\tfrac{1}{4}\alpha_s\frac{(\boldsymbol{\lambda}_i\cdot\boldsymbol{\lambda}_j)}{r_{ij}}, \tag{19}$$

where $\boldsymbol{\lambda}_i$ is the color SU(3) generators for the ith quark, α_s is the strong coupling constant (for this work we used $\alpha_s=0.6$), and r_{ij} is the relative distance between the ith and the jth quarks.

We wish to replace the one-pion exchange (OPE) with the one-gluon exchange at short distances. We will do so with the use of a Gaussian transition function

$$T(r)=e^{-\beta r^2}T_{\mathrm{OGE}}+(1-e^{-\beta r^2})T_{\mathrm{OPE}}. \tag{20}$$

The rms radius of the Gaussian provides a convenient measure of the distance at which the transition takes place, i.e.,

$$R_T=\sqrt{\frac{3}{2\beta}}. \tag{21}$$

We assume that only the S state of the two nucleons is involved so that only the spin-spin part of the one-pion exchange contributes. Thus at small r both OGE and OPE interactions are proportional to $1/r_{ij}$, and the transition between the two interactions in the neighborhood of R_T changes only its strength. (We will keep the momentum carrying part of the propagator e^{ikr} in what follows, but it plays little role at these low energies and short distances.)

Thus the correction to the interaction can be written

$$\Delta T(r)=S_{\mathrm{OPE}}e^{-\beta r^2}(S_{\mathrm{OGE}}/S_{\mathrm{OPE}}-1.0)\frac{e^{ikr}}{r}, \tag{22}$$

where this expression is to be added to the previous OPE result before the correction for the finite size of the nucleon. The quantities S_{OPE} and S_{OGE} are the strengths of the OPE and OGE, respectively. While the true S_{OPE} is known (at least in the present model) the S_{OGE} is more difficult to obtain. We will estimate the ratio in the parenthesis from the ratio that would obtain in the case of a potential.

One gluon cannot be exchanged between two color singlets (such as a pair of nucleons) unless it is accompanied by quark exchange or an additional gluon exchange. This exchange of quarks can be quite complicated but should not be of a small magnitude when the nucleons are strongly overlapping as is the case (most of the time) when the quarks exchanging a gluon are in close proximity. In order to estimate this probability we use the result that there is a hidden color component generated when the nucleons are overlapping [35]. The gluon can then be exchanged between these hidden color components [34].

For the color symmetric pairs the matrix elements $\langle \boldsymbol{\lambda}_i \cdot \boldsymbol{\lambda}_j \rangle$ have been calculated in the physical basis of hidden color states and were found to be equal to $-4/3$ for both $S=0, I=1$ and $S=1, I=0$, the two possible nucleon states for S-wave nucleons [34]. For the OPE the strengths are also the same in these two states.

Hence we can estimate that the ratio

$$S_{\mathrm{OGE}}/S_{\mathrm{OPE}} \simeq \frac{\alpha_s/3}{0.6 f^2/4\pi}, \tag{23}$$

where $f^2/4\pi \simeq 0.0756$ is the pion-nucleon coupling constant and the factor of 0.6 comes from an estimate, with symmetric quark model wave functions, of

$$[f^2/4\pi]_{\mathrm{Quark}} = 0.6[f^2/4\pi]_{\mathrm{Nucleon}}. \tag{24}$$

The ratio of strengths from this estimate is 4.4. We emphasize that this is a very rough number.

The next step is to include the convolution of the propagator with the finite size of the nucleon. To this end we calculate the Fourier transform for the correction, multiply it with the form factor for the nucleon and transform back to coordinate space

$$g_L^{\mathrm{OGE}}(r_1, r_2) \equiv (\alpha^2 + k_0^2)^2 \frac{2}{\pi} \times \int_0^\infty q^2 dq \frac{j_L(qr_1) j_L(qr_2)}{(\alpha^2 + q^2)^2} \Delta T(q). \tag{25}$$

This correction can then be added on in the same manner as the δ-function correction.

C. Results

The results of the short-range correction are shown in Figs. 10–12. The δ-function correction (dot-dashed line) is seen to worsen the agreement with the data on the high-energy side of the peak. The estimate made of the OGE correction tends to restore the agreement, depending on the radius chosen. From the arguments given previously, one expects this distance to correspond to the size of the pion. Of course, a change in the value of the ratio [Eq. (23)] would bring about a corresponding change in the radius obtained, so the reader should be cautioned against drawing any absolute conclusions from the curves. The purpose of this calculation is only to show the order of magnitude of such a correction. One correction that has not been included in the present calculation is the suppression of the short-range nucleon-nucleon wave function due to the strong repulsion at short distances which can be expected to decrease the size of the effect seen here.

V. CONCLUSIONS

We find that the peak in low-energy pion double charge exchange is naturally given by the calculation of the two-step mechanism with realistic distorted waves. The sharper peak obtained in this work than previous work is due to the use of realistic (fitted) pionic wave functions constrained by elastic and reaction data. Corrections to the reaction mechanism that result from the elimination of the unphysical δ function and from an estimate of a short-range quark-quark interaction treated in a one-gluon-exchange approximation are not large but clearly visible in any comparison with the measured cross section.

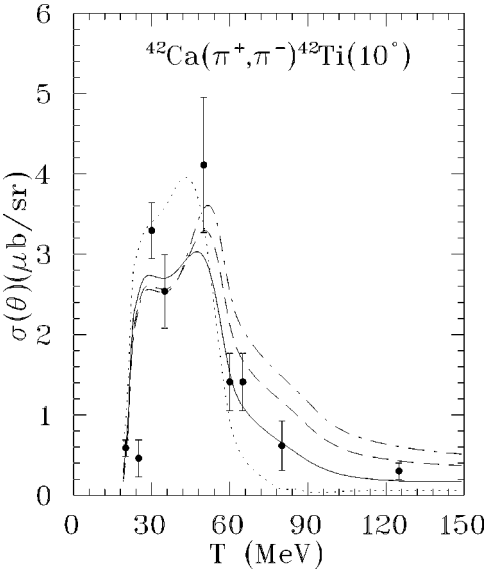

FIG. 10. Cross section for pion double charge exchange on ^{42}Ca leading to the ground state of ^{42}Ti. All of the curves are calculated with the δ-function correction included. The dash-dot curve has this correction alone. The dashed curve has a transition radius of 0.14 fm, the solid curve 0.23 fm, and the dotted curve 0.39 fm.

This work was supported by the U. S. Department of Energy.

APPENDIX A: TECHNIQUE OF CALCULATION

The initial and final pion wave functions are expanded in the usual manner [36] as

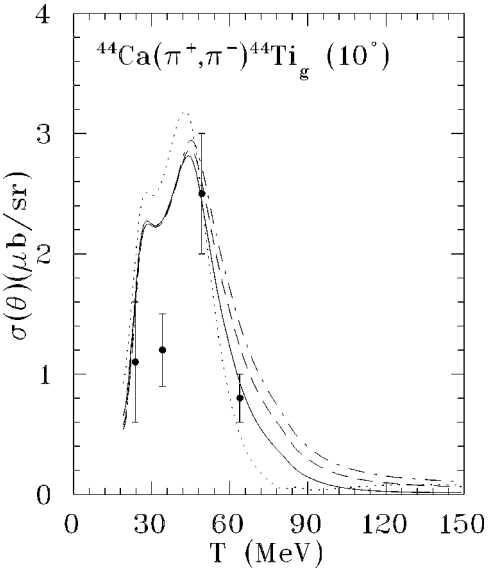

FIG. 11. Cross section for pion double charge exchange on ^{44}Ca leading to the ground state of ^{44}Ti. The meaning of the curves is the same as in Fig. 10.

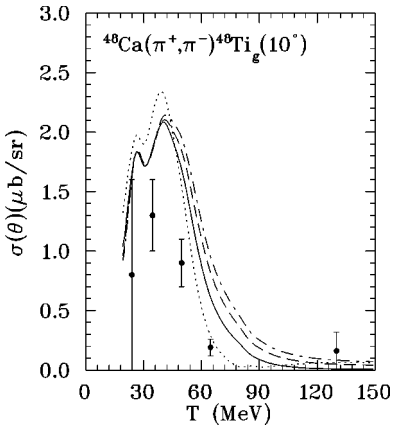

FIG. 12. Cross section for pion double charge exchange on ^{48}Ca leading to the ground state of ^{48}Ti. The meaning of the curves is the same as in Fig. 10.

$$\Psi(\mathbf{k},\mathbf{r}) = 4\pi \sum_{\ell,m=-\ell}^{\ell} i^{\ell} Y_{\ell}^{m*}(\hat{\mathbf{r}}) Y_{\ell}^{m}(\hat{\mathbf{k}}) \psi_{\ell}(k,r). \quad \text{(A1)}$$

The operation of the form factors $v(q)$ on the wave function can be expressed as

$$\tilde{\psi}(\mathbf{k},\mathbf{r}) = \frac{\Lambda^2 + k^2}{\Lambda^2 - \nabla^2} \psi(\mathbf{k},\mathbf{r}). \quad \text{(A2)}$$

Writing the Fourier decomposition for the wave function we have

$$\tilde{\psi}(\mathbf{k},\mathbf{r}) = \frac{\Lambda^2 + k^2}{(2\pi)^3} \int d\mathbf{q}\, d\mathbf{r}' \frac{e^{i\mathbf{q}\cdot(\mathbf{r}'-\mathbf{r})}}{\Lambda^2 + q^2} \psi(\mathbf{k},\mathbf{r}')$$
$$= \frac{\Lambda^2 + k^2}{4\pi} \int d\mathbf{r}' \frac{e^{-\Lambda|\mathbf{r}-\mathbf{r}'|}}{|\mathbf{r}-\mathbf{r}'|} \psi(\mathbf{k},\mathbf{r}'). \quad \text{(A3)}$$

Using the standard expansion of $e^{ik|\mathbf{r}-\mathbf{r}'|}/ik|\mathbf{r}-\mathbf{r}'|$ for imaginary k in terms of the spherical Bessel and Hankel functions, the integral can be calculated partial wave by partial wave, each $\psi_{\ell}(k,r)$ being transformed into $\tilde{\psi}_{\ell}(k,r)$.

Hence each function involved may be transformed as above and then the rest of the calculations performed as if the form factors were not present. The rest of the operators are linear in $\mathbf{q}$ and $\mathbf{q}'$. The dot product of the gradients can be simplified by using the mathematical identity $\mathbf{q}\cdot\mathbf{q}' \equiv \frac{1}{2}[(\mathbf{q}+\mathbf{q}')^2 - q^2 - q'^2]$. The angular momentum algebra for the treatment of the spin-dependent part of the operator is discussed in Ref. [9].

We write the wave function for a given partial wave in the form $\psi_{\ell}(k,r) = C_{\ell} U_{\ell}/r$ since we will first determine the functional form for the radial wave function with arbitrary normalization and separately determine the coefficient C_{ℓ}. The Schrödinger equation for $U_{\ell}(r)$ can be written as

$$U_{\ell}''(r) + \left[\frac{\ell(\ell+1)}{r^2} + \frac{2k\eta}{r}\right] U_{\ell}(r)$$
$$- r\int_0^{\infty} r'\,dr'\, w(r,r') U_{\ell}(r') + k^2 U_{\ell}(r) = 0, \quad \text{(A4)}$$

where

$$w(r,r') \equiv \frac{2\omega}{\hbar^2} V(r,r') \quad \text{(A5)}$$

is calculated by the means of Ref. [16]. Putting the system on a discrete mesh of step ϵ for r and r' we have the following set of equations:

$$\sum_{m=0}^{N} (H_{nm} - k^2 \delta_{nm}) U^m = 0; \quad n = 1,2,...,N-1, \quad \text{(A6)}$$

where $U^n \equiv U(n\epsilon)$. For our calculations a typical value of N was 80.

We require that $U^0 = 0$. This leaves $N-1$ equations in N unknowns. We establish a normalization for the wave function by setting arbitrarily $U^N = 1$. There are now $N-1$ equations in $N-1$ unknowns. The system expressed by Eqs. (A6) is solved by standard numerical techniques to obtain the wave functions for the initial and final pion distorted waves. At this point the true normalization may be obtained from the scattering boundary conditions at infinity.

To compute the Green function which is needed for the propagation between charge exchanges, we first note that, because of its scalar nature, it can be written as

$$\frac{1}{E-H} = G(\mathbf{r}_2,\mathbf{r}_1) = \sum Y_{\ell}^{m*}(\hat{\mathbf{r}}_2) Y_{\ell}^{m}(\hat{\mathbf{r}}_1) G_L(r_2,r_1). \quad \text{(A7)}$$

The spectral representation of a partial wave component of this function will be

$$G_L(r_2,r_1) = 2\omega \int q^2 dq \frac{\psi_L^{(-)}(q,r_2)\psi_L^{(+)}(q,r_1)}{k^2 - q^2}. \quad \text{(A8)}$$

Here $\psi_L^{(+)}(q,r)$ represents a wave function with unit plane wave amplitude and *outgoing* spherical waves while $\psi_L^{(-)}(q,r)$ represents a wave function with unit plane wave amplitude and *incoming* spherical waves. Since the form of $U_L(q,r)$ is uniquely given by the solution of the system of Eqs. (A6), $\psi_L^{(+)}(q,r)$ and $\psi_L^{(-)}(q,r)$ can differ only in normalization.

An inspection of the boundary conditions shows that

$$\psi_L^{(-)}(q,r) = \frac{\psi_L^{(+)}(q,r)}{S_L(q)}, \quad \text{(A9)}$$

which allows the writing of the spectral representation of the Green function as

$$G_L(r_2,r_1)=2\omega\int q^2dq\,\frac{\psi_L(q,r_2)\psi_L(q,r_1)}{S_L(q)(k^2-q^2)}, \quad \text{(A10)}$$

where $\psi_L(q,r)=\psi_L^{(+)}(q,r)$, i.e., the wave function with the usual boundary conditions for scattering. To apply this method the wave functions for the neutral pion must be found for a sufficient range of intermediate momenta and the integral over them performed numerically.

While the spectral representation just given works for many cases (it was used for the calculations in Ref. [9]) it can lead to problems in a region of strong absorption (such as near the Δ resonance in the present case). As has been discussed [37] the S matrix has a series of poles (below the real axis) and zeros (above the real axis in mirror position to the poles for a real potential but above or below the real axis for a complex potential). The zeros will cross the real axis as the imaginary part of the complex potential becomes stronger. That, of course, changes the value of the Green function given by the spectral representation because the singularity due to the zero in $S_L(q)$ passes through the line of integration. In practice this first occurs in the energy region around 120 MeV and the crossing is different for each partial wave. When this happens a discontinuity as a function of energy is observed in the calculated DCX cross section. By deforming the integration contour (numerically) to dip below the real axis, continuity can be restored. However, this method has limited practical application; when the absorption becomes very strong the zero in the S matrix goes far below the real axis and is difficult to locate.

Fortunately, an alternative (and more direct) method exists. Eqs. (A6) provide a matrix representation of $(E\text{-}H)U$. Instead of solving the equations for U it is only necessary to invert the matrix representing $E\text{-}H$. However, we first need to incorporate the boundary conditions. The boundary condition at the origin is the same as before so we can remove, as before, the first column. However the condition at ∞ is different since we now wish to require outgoing spherical waves for large values of r_2. The second derivative in the last equation is the only reference to the last value of the function $U_L(r)$. For purely outgoing waves, we have

$$\frac{U_L^N}{U_L^{N-1}}=\frac{h_L^{(+)}(kr_N)}{h_L^{(+)}(kr_{N-1})}\equiv\beta. \quad \text{(A11)}$$

In both the case for the solution for the wave function and the Green function, the first row refers to the value of the wave function at $r=0$ and the last row refers to the value of the wave function at r_N. Both of these references need to be eliminated to obtain a closed system. Thus by removing the zeroth and Nth equations we have a matrix of size N-1 to invert. The technique of inversion of the matrix was tested against the spectral method and found to give the same result (within numerical accuracy) when the later method was valid.

APPENDIX B: PION ABSORPTION CORRECTION

In the pion absorption process no pion is left in the final state where the pion mass and energy are completely converted to the energy of the nucleons in the final state. The absorption process preferentially involves two or more nucleons to reduce the mismatch between the momentum of the absorbed pion and the Fermi momentum of the nucleons. We approximated the absorption correction by including a purely imaginary term in the optical potential of the form

$$V_{abs}=-iW\rho^2(r), \quad \text{(B1)}$$

where $\rho(r)$ normalized such that $\int_0^\infty r^2dr\,\rho(r)=1$. While perhaps better theories can be invoked [38,39] this method was used for the global fit. The total cross section can be separated into elastic (σ_e), quasifree (σ_{qf}), and true absorption (σ_a) pieces given [38] by

$$\sigma_a=\frac{4\pi W}{k}\sum_l\,(2l+1)\int|\psi_l(r)|^2\rho^2(r)r^2dr, \quad \text{(B2)}$$

$$\sigma_{qf}=-\frac{4\pi}{k}\sum_l\,(2l+1)\times\int\int\psi_l^*(r')\,\mathrm{Im}[V(r,r')]\psi_l(r)r^2dr\,r'^2dr', \quad \text{(B3)}$$

where $V(r,r')$ is the first-order optical potential.

The parameter W was adjusted to reproduce the experimental values for true absorption cross sections for ^{40}Ca (the experimental data [40] were interpolated in mass number). This was done by calculating the absorption cross section (=reaction cross section) with the real part of the quasifree part of the optical potential. By comparing with the data, a value of W can be found at each energy for which data exist. The values of W were fitted to the following formula:

$$W=\frac{W_0(\Gamma/2)^2}{(E-E_0)^2+(\Gamma/2)^2}. \quad \text{(B4)}$$

No particular theoretical importance is attached to this form, it simply gives a good representation of the results. The constants were found to be $W_0=43.35$ fm^4 (for ^{12}C), $E_0=215$ MeV and $\Gamma=77$ MeV. The scaling among nuclei was made assuming that the parameter W_0 was proportional to NZ.

In the process of the fit to the elastic data [17] these values were renormalized. In these fits it was found that the determination of the best value of W_0 for ^{12}C was nearly as predicted by this procedure, but that the value for ^{40}Ca was a factor of 2 too large.

APPENDIX C: THE δ-FUNCTION CORRECTION WITH DISTORTED WAVES

If the distorted pion waves are given by

$$\tilde{\psi}(\mathbf{k},\mathbf{r})=4\pi\sum\,i^\lambda Y_\lambda^{\mu*}(\hat{\mathbf{r}})Y_\lambda^\mu(\hat{\mathbf{k}})\tilde{\phi}_\lambda(k,r) \quad \text{(C1)}$$

the distorted-wave version of the matrix element of the operator defined by Eqs. (17) and (18) is

$$C=-\tfrac{1}{3}(4\pi)^2\int d\mathbf{r_1}d\mathbf{r_2}\chi_f^*(\mathbf{r_1},\mathbf{r_2})\chi_i(\mathbf{r_1},\mathbf{r_2})\mathbf{k_2}\cdot\mathbf{k_1}\sum i^{\lambda-\lambda'}Y_\lambda^{\mu}*(\hat{\mathbf{r}}_1)Y_\lambda^{\mu}(\hat{\mathbf{k}}_i)\tilde{\phi}_\lambda(k_i,r_1)$$
$$\times Y_{\lambda'}^{\mu'}(\hat{\mathbf{r}}_2)Y_{\lambda'}^{\mu'}{}^*(\hat{\mathbf{k}}_f)\tilde{\phi}_{\lambda'}(k_f,r_2)Y_{L'}^{M'}(\hat{\mathbf{r}}_1)Y_{L'}^{M'*}(\hat{\mathbf{r}}_2)g_{L'}(r_1,r_2), \tag{C2}$$

where $\mathbf{k_1}$ and $\mathbf{k_2}$ are to be interpreted as operators acting on the pion wave functions, and $g_L(r_1,r_2)$ is defined in Sec. IV A. For a single shell orbital with angular momentum ℓ and a $0^+\rightarrow 0^+$ transition, the spin average of the nuclear wave function can be written as

$$\langle\chi_f^*(\mathbf{r}_1,\mathbf{r}_2)\chi_i(\mathbf{r}_1,\mathbf{r}_2)\rangle=\chi_\ell^2(r_1)\chi_\ell^2(r_2)\sum a_L Y_L^M(\hat{\mathbf{r}}_1)Y_L^{M*}(\hat{\mathbf{r}}_2), \tag{C3}$$

where the a_L are given by the nuclear shell model [9].

Defining one term in the above sum as $F_L^C(\mathbf{k},\mathbf{k}')$ we have

$$F_L^C(\mathbf{k},\mathbf{k}')=-\tfrac{1}{3}(4\pi)^2\int d\mathbf{r}_1d\mathbf{r}_2\chi_\ell^2(r_1)\chi_\ell^2(r_2)\sum_M Y_L^M(\hat{\mathbf{r}}_1)Y_L^{M*}(\hat{\mathbf{r}}_2)$$
$$\times\sum i^{\lambda-\lambda'}Y_\lambda^{\mu}(\hat{\mathbf{k}}_i)Y_{\lambda'}^{\mu'}{}^*(\hat{\mathbf{k}}_f)Y_{L'}^{M'}(\hat{\mathbf{r}}_1)Y_{L'}^{M'*}(\hat{\mathbf{r}}_2)g_{L'}(r_1,r_2)[\mathbf{k_1}Y_\lambda^{\mu}*(\hat{\mathbf{r}}_1\tilde{\phi}_\lambda(k_i,r_1)\cdot[\mathbf{k_2}Y_{\lambda'}^{\mu'}(\widehat{\mathbf{r_2}})\tilde{\phi}_{\lambda'}(k_f,r_2)]. \tag{C4}$$

Using the definitions

$$F_\lambda(r)=\frac{df_\lambda(r)}{dr}-\frac{\lambda}{r}f_\lambda(r);\quad G_\lambda(r)=\frac{df_\lambda(r)}{dr}+\frac{\lambda+1}{r}f_\lambda(r), \tag{C5}$$

where $f_\lambda(r)$ is either $\tilde{\phi}(k_i,r_1)$ or $\tilde{\phi}(k_f,r_2)$ and

$$f_{\lambda,L}=\int r_1^2dr_1r_2^2dr_2\chi_\ell^2(r_1)\chi_\ell^2(r_2)F_\lambda(r_1)F_\lambda(r_2)g_L(r_1,r_2) \tag{C6}$$

$$g_{\lambda,L}=\int r_1^2dr_1r_2^2dr_2\chi_\ell^2(r_1)\chi_\ell^2(r_2)G_\lambda(r_1)G_\lambda(r_2)g_L(r_1,r_2) \tag{C7}$$

the contribution to the correction can be written as

$$F_L^C=-\tfrac{1}{3}\sum P_\lambda(\cos\theta)\left\{\frac{[C^{0,0,0}_{L,L',\lambda+1}]^2(\lambda+1)^2}{(2\lambda+3)^2}f_{\lambda,L'}+\frac{[C^{0,0,0}_{L,L',\lambda-1}]^2\lambda^2}{(2\lambda-1)^2}g_{\lambda,L'}\right\}. \tag{C8}$$

The calculations for the δ-function correction proceeded by calculating the function $g_L(r_1,r_2)$ analytically and including it in the distorted wave code. The functions $f_{\lambda,L}$ and $g_{\lambda,L}$ were calculated by integrating over r_1 and r_2 using the same nuclear and pion initial and final wave functions and added to the p wave p wave part of the DCX amplitude.

[1] M. J. Leitch *et al.*, Phys. Lett. B **294**, 157 (1992).

[2] M. J. Leitch, *et al.*, Phys. Rev. C **39**, 2356 (1983).

[3] R. Bilger, H. Clement, and M. G. Schepkin, Phys. Rev. Lett. **71**, 42 (1993); **72**, 2972 (1994).

[4] W. R. Gibbs, W. B. Kaufmann, and J.-P. Dedonder, Phys. Lett. B **231**, 6 (1989).

[5] N. Auerbach, in *Proceedings of the LAMPF Users Group Symposium*, edited by B. F. Gibson, C. M. Hoffman, P. D. Barnes, and V. W. Hughes (World Scientific, Singapore, 1997), p. 47.

[6] M. A. Kagarlis and M. B. Johnson, Phys. Rev. Lett. **73**, 38 (1994).

[7] M. B. Johnson, E. Oset, H. Sarafian, E. R. Siciliano, and M. Vicente-Vacas, Phys. Rev. C **44**, 2480 (1991).

[8] Y. Liu, A. Faessler, J. Schwieger, and A. Bobyk, J. Phys. G **24**, 1135 (1998).

[9] N. Auerbach, W. R. Gibbs, J. N. Ginocchio, and W. B. Kaufmann, Phys. Rev. C **38**, 1277 (1988).

[10] N. Auerbach, W. R. Gibbs, and E. Piasetzky, Phys. Rev. Lett. **59**, 1076 (1987).

[11] E. Bleszynski, M. Bleszynski, and R. J. Glauber, Phys. Rev. Lett. **60**, 1483 (1988); T. Karapiperis and M. Kobayashi, *ibid.* **54**, 1230 (1985); W. R. Gibbs, J. N. Ginocchio, and N. Auerbach, Comments Nucl. Part. Phys. **20**, 141 (1991).

[12] E. R. Siciliano, M. B. Johnson, and H. Sarafian, Ann. Phys. (N.Y.) **203**, 1 (1990).
[13] M. F. Jiang and D. S. Koltun, Phys. Rev. C **42**, 2662 (1990); E. Oset, D. S. Strottman, M. J. Vicente-Vacas, and J. Wei-Hsing, Nucl. Phys. **A408**, 461 (1983).
[14] E. Oset, M. J. Vicente-Vacas, M. B. Johnson, D. Strottman, H. T. Fortune, and R. Gilman, Nucl. Phys. **A483**, 514 (1988).
[15] E. Oset, M. Khankhasayev, J. Nieves, H. Sarafian, and M. J. Vicente-Vacas, Phys. Rev. C **46**, 2406 (1992).
[16] W. B. Kaufmann and W. R. Gibbs, Phys. Rev. C **28**, 1286 (1983).
[17] M. Nuseirat, M. A. K. Lodhi, and W. R. Gibbs, Phys. Rev. C **58**, 314 (1998).
[18] W. R. Gibbs, W. B. Kaufmann, and P. B. Siegel, in Proceedings of the LAMPF Workshop on Pion Double Charge Exchange, Los Alamos Report No. LA-10550-C(1985), p. 90.
[19] H. Sarafian, M. B. Johnson, and E. R. Siciliano, Phys. Rev. C **48**, 1988 (1993).
[20] M. K. Khankhasayev, H. Sarafian, M. B. Johnson, and Z. B. Kurmanov, Phys. Rev. C **50**, 1424 (1994).
[21] W. B. Kaufmann, Jane C. Jackson, and W. R. Gibbs, Phys. Rev. C **9**, 1340 (1974).
[22] J. D. McCullen, B. F. Bayman, and L. Zamick, Princeton University Technical Report No. NYO-9891, 1964 (unpublished); Phys. Rev. **134**, B515 (1964); J. N. Ginocchio, Phys. Rev. **144**, 952 (1966); J. N. Ginocchio and J. B. French, Phys. Lett. **7**, 137 (1963); See Ref. [9] for the application of these wave functions to pion DCX.
[23] W. R. Gibbs, M. Elghossain, and W. B. Kaufmann, Phys. Rev. C **48**, 1546 (1993).
[24] W. R. Gibbs and B. Loiseau, Phys. Rev. C **50**, 2742 (1994).
[25] M. Ericson and T. E. O. Ericson, Ann. Phys. (N.Y.) **36**, 323 (1966).
[26] G. Baym and G. E. Brown, Nucl. Phys. **A247**, 395 (1975).
[27] Below 80 MeV the single charge exchange amplitudes were taken from P. B. Siegel and W. R. Gibbs, Phys. Rev. C **33**, 1407 (1986). Above that energy values calculated from the phase shifts of M. Rowe, M. Solomon, and R. Landau, *ibid.* **18**, 584 (1978) were used.
[28] J. N. Ginocchio, Nucl. Phys. **A560**, 321 (1993); Phys. Rev. C **48**, 1460 (1993).
[29] W. B. Kaufmann and W. R. Gibbs, in Proceedings of the *Second LAMPF International Workshop on Pion-nucleus Double Charge Exchange*, 1989. edited by W. R. Gibbs and M. J. Leitch (World Scientific, Singapore, 1990), p. 135.
[30] S. Cohen and D. Kurath, Nucl. Phys. **73**, 1 (1965).
[31] R. Gilman *et al.*, Phys. Rev. C **35**, 1334 (1987).
[32] M. Kaletka *et al.*, Phys. Lett. B **199**, 336 (1987).
[33] P. A. Seidl *et al.*, Phys. Rev. C **42**, 1929 (1990).
[34] A. Faessler *et al.*, Nucl. Phys. **A402**, 555 (1983).
[35] M. Harvey, Nucl. Phys. **A352**, 301 (1980); **A352**, 326 (1980).
[36] W. R. Gibbs, *Computation in Modern Physics* (World Scientific, Singapore, 1994).
[37] Discussions of the effect of the zeros in the *S* matrix can be found in W. R. Gibbs, Phys. Rev. C **27**, 408 (1983); Phys. Lett. B **103**, 281 (1981); Phys. Rev. **181**, 1414 (1969).
[38] H. Garcilazo and W. R. Gibbs, Nucl. Phys. **A381**, 487 (1982).
[39] J. Nieves, E. Oset, and C. Garcia-Recio, Nucl. Phys. **A554**, 554 (1993).
[40] D. Ashery *et al.*, Phys. Rev. Lett. **23**, 2173 (1980); K. Nakai *et al.*, *ibid.* **44**, 1446 (1980); R. D. Ransome *et al.*, Phys. Rev. C **46**, 273 (1992); D. Ashery, I. Navon, G. Azuelos, H. K. Walter, H. J. Pfeiffer, and F. W. Schlepütz, *ibid.* **23**, 2173 (1981).